

RAYS OF POLYNOMIAL MAXIMAL SURFACES IN AdS_3

CHUMENG DI, ETHAN LEVIN, AND ARIE OGRANOVICH

1. INTRODUCTION

A key object of study in mathematical physics is anti-de Sitter space, a class of manifolds that provides an important theoretical framework for several prominent fields. Most useful when applied to the General Theory of Relativity, it acts as a solution to the set of PDE's known as the Einstein Field Equations which govern the universal geometry of all spacetime. In particular, this gives a model which accommodates for the observed accelerating expansion famous in cosmology, predicting a slight negative curvature in regions with little to no energy or mass present. It's applications also extend to the AdS/CFT correspondence, a major theoretical coupling between quantum gravity (the extension of general relativity onto quantum scales) and quantum field theory (describing the interaction of quantum mechanics to field theories such as electromagnetism).

Previous research [Tam19] has established a homeomorphism between the space of maximal surfaces (i.e. with zero mean curvature) in anti-de Sitter space and polynomial quadratic differentials over \mathbb{C} . In this project we studied the limiting behavior of this correspondence by fixing a polynomial $p(z)$, and studying the surface associated with $tp(z)dz^2$ as $t \in \mathbb{R}$ tends to infinity.

To accomplish this, we first created a program which takes as input a polynomial quadratic differential over \mathbb{C} and outputs the image of the corresponding maximal surface in AdS_3 .

By studying examples generated by this program, we were able to formulate and prove the following result:

Theorem A. *Let $q = p(z)dz^2$ be a polynomial quadratic differential. There exists a non-negative integer k so that the surface associated with tq converges to the surface associated with $w^k dw^2$ as $t \in \mathbb{R}$ tends to infinity.*

2. ANTI-DE SITTER SPACE

anti-de Sitter space is an n -dimensional manifold endowed with a Lorentzian structure. In this paper, we will work with 3-dimensional anti-de Sitter space, denoted \widehat{AdS}_3 , which is topologically a torus. We can realize it in \mathbb{R}^4 as the set of points satisfying $\langle x, x \rangle = -1$,

Date: July 30, 2021.

where $\langle x, y \rangle := x_1y_1 + x_2y_2 - x_3y_3 - x_4y_4$. In the next section we will study maximal surfaces in \widehat{AdS}_3 , which are the surfaces with zero mean curvature.

Our goal will be to visualize a maximal surface from \widehat{AdS}_3 in 3 dimensions. Up to transformation by an element of $SO(2, 2) = \text{Isom}(\text{AdS}_3)$, every maximal surface in anti-de Sitter space is equivalent to a maximal surface all of whose points have nonzero last coordinate. We can project this into \mathbb{RP}^3 , and finally visualize \mathbb{RP}^3 minus all points with last coordinate 0 as \mathbb{R}^3 .

We denote by AdS_3 the projection of \widehat{AdS}_3 into \mathbb{RP}^3 . If we consider only the projection $\mathbb{P}(\widehat{AdS}_3 \setminus \{x \in \widehat{AdS}_3 : x_4 = 0\})$, ignoring the slice of AdS_3 with 4th coordinate equal to 0, we can visualize this subset of AdS_3 in \mathbb{R}^3 by scaling each point so that the 4th coordinate is equal to 1; then we can parametrize the resulting surface using only the first 3 coordinates. With such a parametrization, we visualize AdS_3 in the following way.

Proposition 2.1. *Consider the embedding of $\mathbb{P}(\widehat{AdS}_3 \setminus \{x \in \widehat{AdS}_3 : x_4 = 0\})$ in \mathbb{R}^3 found by scaling each coordinate so that $x_4 = 1$, and subsequently projecting onto the first three coordinates. Then the image of this embedding is $\{(x, y, z) \in \mathbb{R}^3 : x^2 + y^2 - z^2 < 1\}$.*

Proof. We will first prove that the image of this projection is a subset of $\{(x, y, z) \in \mathbb{R}^3 : x^2 + y^2 - z^2 < 1\}$, and then we will prove the image contains $\{(x, y, z) \in \mathbb{R}^3 : x^2 + y^2 - z^2 < 1\}$.

Let $x = [x_1, x_2, x_3, x_4] \in \mathbb{P}(\widehat{AdS}_3)$ be given so that $x_4 \neq 0$. Then

$$[x_1, x_2, x_3, x_4] = \left[\frac{x_1}{x_4}, \frac{x_2}{x_4}, \frac{x_3}{x_4}, 1 \right].$$

in \mathbb{RP}^3 , hence we can describe these points using the coordinates $(x_1/x_4, x_2/x_4, x_3/x_4)$ in \mathbb{R}^3 . Now, observe that

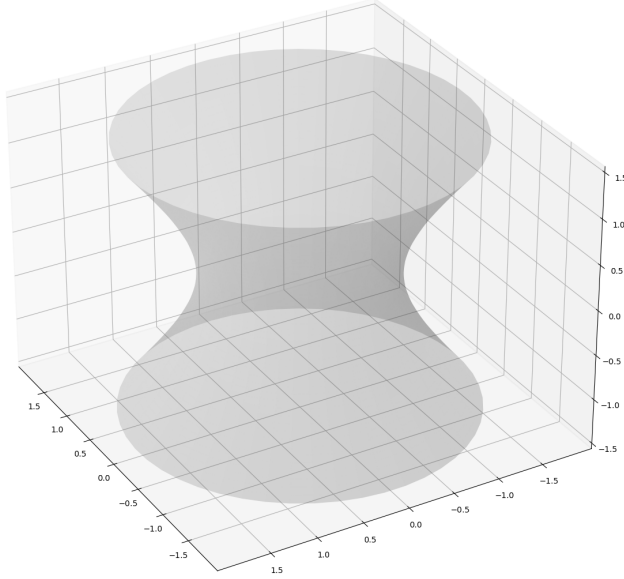
$$\left(\frac{x_1}{x_4}\right)^2 + \left(\frac{x_2}{x_4}\right)^2 - \left(\frac{x_3}{x_4}\right)^2 - 1 = \frac{1}{x_4^2}(x_1^2 + x_2^2 - x_3^2 - x_4^2) = \frac{-1}{x_4^2}$$

since $\langle x, x \rangle = -1$. From this we can conclude

$$\left(\frac{x_1}{x_4}\right)^2 + \left(\frac{x_2}{x_4}\right)^2 - \left(\frac{x_3}{x_4}\right)^2 = 1 - \frac{1}{x_4^2} < 1.$$

In the other direction, let $(x, y, z) \in \mathbb{R}^3$ be given so that $x^2 + y^2 - z^2 < 1$. Then $x^2 + y^2 - z^2 - 1 = -w^2$ for some $w^2 \in \mathbb{R}_+$. Let $x' = (x/w, y/w, z/w, 1/w)$. We can verify that $\langle x', x' \rangle = -1$, so $x' \in \widehat{AdS}_3$. Then $\mathbb{P}(x') = [x, y, z, 1]$, which clearly maps to (x, y, z) under our projection, giving us a preimage of each (x, y, z) . This concludes the proof. \square

This means that, in visualizing surfaces and boundaries of maximal surfaces, our visualizations will live inside the hyperboloid in Figure 1. In the next section, we explicitly introduce maximal surfaces and study the correspondence between these surfaces and polynomial quadratic differentials.


 FIGURE 1. Visualization of AdS_3 in \mathbb{R}^3 .

3. MAXIMAL SURFACES IN ANTI-DE SITTER SPACE

A maximal surface in anti-de Sitter space can be defined in an analogous fashion to a minimal surface in \mathbb{R}^3 . First, let $f : \Omega \subseteq \mathbb{C} \rightarrow \widehat{AdS}_3$ be a smooth map, and let $S := f(\Omega)$ be the corresponding surface. We may associate to every $p \in \Omega$ its tangent plane $T_{f(p)}S$, of which $\{f_x(p), f_y(p)\}$ is a basis. Then, the symmetric bilinear form $\langle \cdot, \cdot \rangle$ restricts to a bilinear form on $T_{f(p)}S$. If this bilinear form is positive definite, then $T_{f(p)}S$ becomes an inner product space with respect to this product. This leads us to the following definition:

Definition 3.1. Let $f : \Omega \subseteq \mathbb{C} \rightarrow \widehat{AdS}_3$ be a smooth function, and let $S := f(\Omega)$ be the corresponding surface. We say that S is *space-like* if for all $p \in \Omega$ and all $v \in T_{f(p)}S$, $\langle v, v \rangle \geq 0$, with equality if and only if $v = 0$.

Now, we can define the first and second fundamental forms of S , which are common tools in studying the differential geometry of surfaces. We begin with the first fundamental form:

Definition 3.2 (First Fundamental Form). Let $f : \Omega \subseteq \mathbb{C} \rightarrow \widehat{AdS}_3$ be a smooth function, and let $S := f(\Omega)$ be the corresponding surface. The first fundamental form of S is the map $I : T_{f(p)}S \times T_{f(p)}S \rightarrow \mathbb{R}$ so that $I(v, w) = \langle v, w \rangle$. We can encode I as the following matrix, using the basis $\{f_x(p), f_y(p)\}$:

$$I = \begin{pmatrix} \langle f_x(p), f_x(p) \rangle & \langle f_x(p), f_y(p) \rangle \\ \langle f_x(p), f_y(p) \rangle & \langle f_y(p), f_y(p) \rangle \end{pmatrix}.$$

With this definition, we can check if S is space-like by checking if I is positive definite. This allows us to make precise a notion of angle-preserving, as follows:

Definition 3.3. Let $f : \Omega \subseteq \mathbb{C} \rightarrow \widehat{AdS}_3$ be a smooth function, and let $S := f(\Omega)$ be the corresponding surface. We say that f is *conformal* if

$$I = \begin{pmatrix} 2e^{2u} & 0 \\ 0 & 2e^{2u} \end{pmatrix},$$

or, equivalently, if $I = 2e^{2u}(dx^2 + dy^2) = 2e^2|dz|^2$.

Clearly if f is conformal then I is positive definite, so S is space-like. When f is conformal it will be convenient to normalize f_x and f_y by introducing the following vectors:

$$\sigma_1 = \frac{f_x}{e^u\sqrt{2}}, \quad \sigma_2 = \frac{f_y}{e^u\sqrt{2}}.$$

Using these, we can also introduce a unit normal vector, denoted N , which is orthogonal to each of σ_1, σ_2 , and f , and also satisfies $\det(\sigma_1, \sigma_2, f, N) = 1$. We know such an N exists by choosing the orthogonal vector to these 3 that maintains positive orientation and using Gram Schmidt to complete an orthonormal basis, and we specify the orientation via the determinant condition.

We also introduce the second fundamental form here:

Definition 3.4 (Second Fundamental Form). Let $B : T_{f(p)}S \rightarrow T_{f(p)}S$ denote the shape operator, in other words $B(v) = \partial N / \partial v$. We define the second fundamental form $\mathbb{I}(v, w) = I(B(v), w)$.

Using these fundamental forms, we can study the mean curvature of surfaces in \widehat{AdS}_3 . A maximal surface will be a space-like surface with zero mean curvature. For the purpose of this paper, we define such surfaces as follows:

Definition 3.5 (Maximal Surface). We say that a space-like surface $S \subseteq \widehat{AdS}_3$ is *maximal* when $\text{trace}(\mathbb{I}) = 0$.

The basis $\{\sigma_1, \sigma_2, N, f\}$ of \mathbb{R}^4 is orthogonal with respect to the inner product $\langle \cdot, \cdot \rangle$ of signature $(2, 2)$: we know σ_1 and σ_2 are orthogonal to each other since f is conformal. We also know f is orthogonal to σ_1 and σ_2 since for any vector $v \in T_{f(p)}S$,

$$\langle f, \partial f / \partial v \rangle = \frac{1}{2} \frac{\partial}{\partial v} \langle f, f \rangle = \frac{1}{2} \frac{\partial}{\partial v} (1) = 0.$$

Finally, we know N is orthogonal to the other three vectors by construction. Thus, $\{\sigma_1, \sigma_2, N, f\}$ is an orthogonal basis of \mathbb{R}^4 .

This lets us write any vector v in components as follows:

$$v = \langle v, \sigma_1 \rangle \sigma_1 + \langle v, \sigma_2 \rangle \sigma_2 + \langle v, f \rangle f + \langle v, N \rangle N,$$

which allows us to evaluate the derivative of each basis element in terms of the other elements and the requirement $\text{trace}(\mathbb{I}) = 0$ fairly easily. Computation reveals the following:

$$\begin{aligned}
 (\sigma_1)_x &= 0\sigma_1 - u_y\sigma_2 + (e^{-u}/\sqrt{2})\mathbb{I}_{1,1}N + e^u\sqrt{2}f \\
 (\sigma_2)_x &= u_y\sigma_1 + 0\sigma_2 + (e^{-u}/\sqrt{2})\mathbb{I}_{1,2}N + 0f \\
 N_x &= (e^{-u}/\sqrt{2})\mathbb{I}_{1,1}\sigma_1 + (e^{-u}/\sqrt{2})\mathbb{I}_{1,2}\sigma_2 + 0N + 0f \\
 f_x &= e^u\sqrt{2}\sigma_1 + 0\sigma_2 + 0N + 0f \\
 (\sigma_1)_y &= 0\sigma_1 + u_x\sigma_2 + (e^{-u}/\sqrt{2})\mathbb{I}_{1,2}N + 0f \\
 (\sigma_2)_y &= -u_x\sigma_1 + 0\sigma_2 - (e^{-u}/\sqrt{2})\mathbb{I}_{1,1}N + e^u\sqrt{2}f \\
 N_y &= (e^{-u}/\sqrt{2})\mathbb{I}_{1,2}\sigma_1 - (e^{-u}/\sqrt{2})\mathbb{I}_{1,1}\sigma_2 + 0N + 0f \\
 f_y &= 0\sigma_1 + e^u\sqrt{2}\sigma_2 + 0N + 0f
 \end{aligned}$$

We can condense these equations by introducing the matrix \mathcal{F} , whose columns are σ_1, σ_2, N, f in order. The above equations then reduce to the following two equations:

$$\partial_x \mathcal{F} = \mathcal{F} \begin{pmatrix} 0 & u_y & (e^{-u}/\sqrt{2})\mathbb{I}_{1,1} & e^u\sqrt{2} \\ -u_y & 0 & (e^{-u}/\sqrt{2})\mathbb{I}_{1,2} & 0 \\ (e^{-u}/\sqrt{2})\mathbb{I}_{1,1} & (e^{-u}/\sqrt{2})\mathbb{I}_{1,2} & 0 & 0 \\ e^u\sqrt{2} & 0 & 0 & 0 \end{pmatrix} \quad (3.1)$$

$$\partial_y \mathcal{F} = \mathcal{F} \begin{pmatrix} 0 & -u_x & (e^{-u}/\sqrt{2})\mathbb{I}_{1,2} & 0 \\ u_x & 0 & -(e^{-u}/\sqrt{2})\mathbb{I}_{1,1} & e^u\sqrt{2} \\ (e^{-u}/\sqrt{2})\mathbb{I}_{1,2} & -(e^{-u}/\sqrt{2})\mathbb{I}_{1,1} & 0 & 0 \\ 0 & e^u\sqrt{2} & 0 & 0 \end{pmatrix} \quad (3.2)$$

In general, we have the following requirement for integrability of a system of ODEs:

Theorem 3.6. *If there is a system of differential equations $\partial_x M = MP$ and $\partial_y M = MQ$, then there exists a solution to M if and only if $Q_x - P_y = QP - PQ$.*

Then, if S is a maximal surface, the above system is integrable. If we check the integrability condition, we reduce a system of equations to get that

$$\begin{aligned}
 \Delta u &= -\frac{1}{2}e^{2u}(\mathbb{I}_{1,1}^2 + \mathbb{I}_{1,2}^2) + 2e^{2u} \\
 (\mathbb{I}_{1,2})_x &= (\mathbb{I}_{1,1})_y \\
 (-\mathbb{I}_{1,1})_x &= (\mathbb{I}_{1,2})_y.
 \end{aligned}$$

The last two equations are the Cauchy-Riemann equations for a holomorphic function. In other words, these last two equations are true if and only if there is a holomorphic quadratic differential $q = h(z)dz^2$, where $h : \Omega \rightarrow \mathbb{C}$ is holomorphic, so that

$$\mathbb{I} = 2\mathcal{R}e(q) = \begin{pmatrix} 2\mathcal{R}e(h) & -2\text{Im}(h) \\ -2\text{Im}(h) & -2\mathcal{R}e(h) \end{pmatrix} \quad (3.3)$$

This allows us to also rewrite the first of those 3 equations in terms of q :

$$\begin{aligned} \Delta u &= -\frac{1}{2}e^{2u}(\mathbb{I}_{1,1}^2 + \mathbb{I}_{1,2}^2) + 2e^{2u} \\ &= -\frac{1}{2}e^{2u}(4\mathcal{R}e(h)^2 + 4\text{Im}(h)^2) + 2e^{2u} \\ &= 2e^{2u} - 2e^{2u}|q|^2. \end{aligned} \quad (3.4)$$

In conclusion, if S is a maximal surface, then equations (3.1), (3.2), (3.3), and (3.4) are all satisfied. The converse is clearly also true, since if S is a space-like surface that obeys (2.3), the trace of its second fundamental form must be 0.

We just found q given f , but we can also go backwards. If we are given a holomorphic quadratic differential q , we can solve (3.4) for u , which determines the coefficients of the matrices in (3.1) and (3.2). Then we can solve the system (3.1) and (3.2) for \mathcal{F} ; the last column of \mathcal{F} gives us f , hence allowing us to uniquely determine S from q . This demonstrates a bijection between the space of holomorphic quadratic differentials on \mathbb{C} and the space of maximal surfaces in \widehat{AdS}_3 . As shown in [Tam19], this bijection is a homeomorphism.

4. CONVERGENCE OF POLYNOMIAL MAXIMAL SURFACES

We consider a ray of holomorphic quadratic differentials q_t and denote by u_t the solution of the PDE

$$\Delta u_t = 2e^{2u_t} - 2e^{-2u_t}|q_t|^2,$$

where for each t the solution exists and is unique. We want to understand the behavior of u_t as $t \rightarrow \infty$ in a neighborhood of the origin. Our ultimate goal is to find a limiting surface (or, a limit equivalent up to transformations in $\text{SO}(2, 2)$) described by u_t as t tends to infinity.

To this end, our program produced numerous examples of maximal surfaces generated by polynomials, and visually demonstrated how the surfaces evolve when t grows large. For the most part, our program computed the boundary of the surfaces as opposed to the surfaces themselves, since visualizing the entire surface tended to be computationally expensive and each boundary corresponds to a unique surface.

The program itself had several key processes in producing such surfaces. For the purposes of this paper, we chose to center our polynomials about the origin. As we will see in Lemma

4.3, this meant transforming all inputed polynomials to be monic and centered would be most beneficial. To continue however, it must find a solution to the PDE (3.4). It does so by perturbing an initial input function, which we may derive as $\frac{1}{4} \log(|q|^2)$ through the next two lemmas.

Lemma 4.1. *Let $v = \mu - \frac{1}{4} \log(|q|^2)$ where μ is the solution to our initial PDE. Then as $|z| \rightarrow +\infty$, we have $v \rightarrow 0$.*

Proof. We first note that because $\frac{1}{4} \log(|q|^2)$ is only defined outside of the zeroes of our polynomial q , wherein we have $T(\frac{1}{4} \log(|q|^2)) = \Delta(\frac{1}{4} \log(|q|^2))$. Noting also that this function goes to $-\infty$ as it approaches one of those zeroes, then by the Cheng-Yau Maximum Principle, we have that $\frac{1}{4} \log(|q|^2) \leq \mu$. By Lemma 3.2, we have then that

$$\begin{aligned} 0 &\leq \mu - \frac{1}{4} \log(|q|^2) \\ &\leq \frac{1}{4} \log(|q|^2 + C) - \frac{1}{4} \log(|q|^2) \\ &= \frac{1}{4} \log\left(\frac{|q|^2 + C}{|q|^2}\right) \rightarrow 0 \quad \text{as } |z| \rightarrow +\infty \end{aligned}$$

as desired. \square

Lemma 4.2. *There exists a constant $C > 0$ such that the function $\mu^+ = \frac{1}{4} \log(|q|^2 + C)$ has the property that $0 \leq \Delta\mu^+ \leq 2e^{2\mu^+} - 2e^{-2\mu^+} |q|^2 = T(\mu^+)$. This inequality also implies $\mu \leq \mu^+$.*

Proof. We begin by finding $\Delta\mu^+$ and $T(\mu^+)$, which we can find by explicitly calculating them:

$$\begin{aligned} \Delta\mu^+ &= \partial_z \partial_{\bar{z}} \log(|q|^2 + C) \\ &= \partial_z \left(\frac{q \bar{q}_{\bar{z}}}{|q|^2 + C} \right) \\ &= \frac{q_z \bar{q}_{\bar{z}} (|q|^2 + C) - q_z \bar{q} q \bar{q}_{\bar{z}}}{(|q|^2 + C)^2} \\ &= \frac{|q_z|^2 C}{(|q|^2 + C)^2} > 0 \end{aligned}$$

as $C > 0$ by construction and because both other terms are squares of real values. Next, we find that

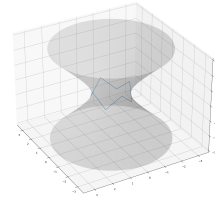
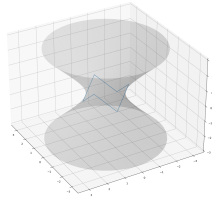
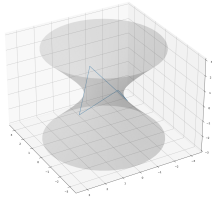
$$\begin{aligned} T(\mu^+) &= 2e^{2\mu^+} - 2e^{-2\mu^+} |q|^2 = 2(|q|^2 + C)^{\frac{1}{2}} - 2(|q|^2 + C)^{-\frac{1}{2}} |q|^2 \\ &= \frac{2(|q|^2 + C) - 2|q|^2}{(|q|^2 + C)^{\frac{1}{2}}} \end{aligned}$$

$$= \frac{2C}{(|q|^2 + C)^{\frac{1}{2}}}.$$

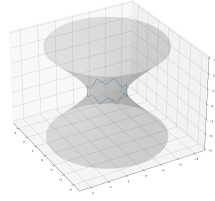
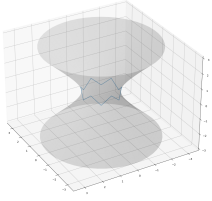
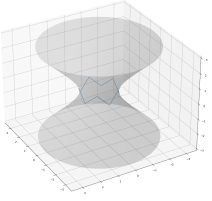
We can now look for a $C > 0$ such that $\Delta\mu^+ \leq T(\mu^+)$ which is equivalent to saying $|q_z|^2 C \leq 2C(|q|^2 + C)^{\frac{3}{2}}$. This is clearly satisfied for large C , since the left hand side grows at the order of C while the right hand side grows at the order of $C^{5/2}$. To prove that $\mu \leq \mu^+$, we simply invoke the Cheng-Yau Maximum Principle. \square

Once it has obtained a solution through perturbation of this test function, it then goes onto integrating along the solution to the ODE's (3.1) and (3.2). By calculating the largest eigenvalue to the resulting matrix, the associated eigenvector then gives the vertices of the polygon representing the boundary of the surface, when we integrate the ODEs along the lines through the origin with direction $\frac{k\pi}{n+2}$, for $k = 1, \dots, 2(n+2)$, where n is the degree of the polynomial.

To calculate the actual surface, the process is similar, however requires integrating on a fine grid to be accurately depicted, which as mentioned, is far more time expensive. These are then mapped onto the 3D representation of anti-de Sitter space described in Section 2.

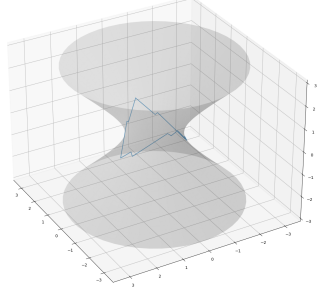
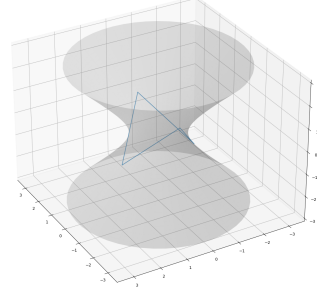
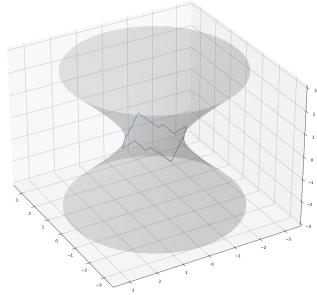
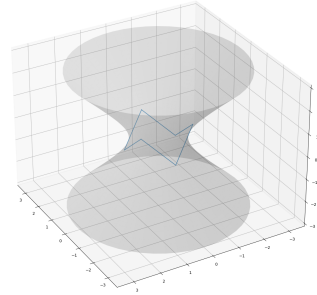


(A) Boundary for $p(z) = 1$ (B) Boundary for $p(z) = z$ (C) Boundary for $p(z) = z^2$



(D) Boundary for $p(z) = z^3$ (E) Boundary for $p(z) = z^4$ (F) Boundary for $p(z) = z^5$

Finally, we used our program to study the behavior of the polygons corresponding to the rays $tp(z)dz^2$ as $t \in \mathbb{R}$ goes to $+\infty$. We denote by S_t the corresponding maximal surfaces. We discovered that the limiting configuration depends on the order of $0 \in \mathbb{C}$ as root of $p(z)$, as the following examples show.


 (A) Boundary for $p(z) = z^5 + 1$

 (B) Boundary for $p(z) = 30000(z^5 + 1)$

 (A) Boundary for $p(z) = z^5 + z$

 (B) Boundary for $p(z) = 30000(z^5 + z)$

Lemma 4.3. *Let $q_t = tq_0$ with $q_0 = (z^n + a_{n-2}z^{n-2} + \dots + a_kz^k)dz^2$. There is a unique $\alpha > 0$ such that in the coordinate $w = (a_k t)^\alpha z$ we have $q_t = \hat{q}_t(w)dw^2 \rightarrow w^k dw^2$ as $t \rightarrow \infty$.*

Proof. We begin by choosing the coordinate $w = (a_k t)^\alpha z$ to write the quadratic differential q_t , giving us

$$\begin{aligned} q_t &= t \left(\frac{w^n}{t^{n\alpha} a_k^{n\alpha}} + \frac{a_{n-2} w^{n-2}}{t^{(n-2)\alpha} a_k^{(n-2)\alpha}} + \dots + \frac{a_k w^k}{t^{k\alpha} a_k^{k\alpha}} \right) \frac{dw^2}{a_k^{2\alpha} t^{2\alpha}} \\ &= \left(\frac{a_k^{-(n+2)\alpha} w^n}{t^{(n+2)\alpha-1}} + \frac{a_{n-2} w^{n-2}}{a_k^{n\alpha} t^{n\alpha-1}} + \dots + \frac{a_k^{-(k+2)\alpha+1} w^k}{t^{(k+2)\alpha-1}} \right) dw^2 \\ &= \hat{q}_t(w) dw^2 \end{aligned}$$

Now, we notice that if we choose α to be $\frac{1}{k+2}$, then this eliminates the factor of t in the coefficient of w^k , but keeps all other coefficients inversely proportional to a positive power of t . This means that as we scale t to infinity, all other coefficients go to 0, and thus we are left with $\lim_{x \rightarrow +\infty} \hat{q}_t(w)dw^2 = w^k dw^2$, as desired. \square

Theorem 4.4. *In a neighborhood of $0 \in \mathbb{C}$, the solutions u_t converge as $t \rightarrow +\infty$ to the unique solution of the equation*

$$\Delta v = 2e^{2v} - 2e^{-2v}|w|^{2k},$$

where k is the order of $0 \in \mathbb{C}$ as root of q_0 .

Proof. Let $q_t = tq_0 = t(z^n + a_{n-2}z^{n-2} + \dots + a_k z^k)dz^2$. Consider the ball

$$B_\epsilon(0) = \{z \in \mathbb{C} \mid |z| < \epsilon\}$$

We change coordinates and let $w = (a_k t)^\alpha z$ as in Lemma 4.3. We rewrite the equation of u_t in this new coordinate. We set

$$I = 2e^{2u_t}|dz|^2 = 2e^{2v_t}|dw|^2 = 2e^{2v_t}|a_k|^{2\alpha}t^{2\alpha}|dz|^2 \quad (4.1)$$

We take the logarithm and get

$$u_t(z) = v_t(w) + \frac{1}{2} \log(|a_k|^{2\alpha}t^{2\alpha}) \quad (4.2)$$

The Laplacian in the new coordinate z can be written as

$$\Delta_z = 4 \frac{\partial}{\partial z} \frac{\partial}{\partial \bar{z}} = 4a_k^\alpha t^\alpha \frac{\partial}{\partial w} (\bar{a}_k)^\alpha (\bar{t})^\alpha \frac{\partial}{\partial \bar{w}} = |a_k|^{2\alpha} t^{2\alpha} \Delta_w. \quad (4.3)$$

Note that

$$q_t(z)dz^2 = q_t((a_k t)^{-\alpha} w)(a_k t)^{-2\alpha} dw^2. \quad (4.4)$$

Taking the modulus squared we get

$$|q_t(z)|^2 = |q_t((a_k t)^{-\alpha} w)|^2 |a_k t|^{-4\alpha} = |\hat{q}_t(w)|^2 \quad (4.5)$$

Since $\Delta_z u_t = 2e^{2u_t} - 2e^{-2u_t}|q_t(z)|^2$, by (4.2), (4.3) we get

$$|a_k|^{2\alpha} t^{2\alpha} \Delta_w v_t = 2e^{2v_t} (|a_k|t)^{2\alpha} - 2e^{-2v_t} (|a_k|t)^{-2\alpha} |q_t((a_k t)^{-\alpha} w)|^2$$

By (4.5) we get

$$\Delta_w v_t = 2e^{-2v_t} - 2e^{-2v_t} |\hat{q}_t(w)|^2. \quad (4.6)$$

By Lemma 4.3, $\hat{q}_t(w)dw^2 \rightarrow w^k dw^2$ as $t \rightarrow \infty$, hence, taking the limit in (4.6) we see that v_t converges to the solution of

$$\Delta v = 2e^{2v} - 2e^{-2v}|w|^{2k}$$

as desired. \square

By Theorem 4.4, the solutions to PDE $v_t(w)$ converge to $v(w)$ as $t \rightarrow +\infty$, so the induced metrics $I_t = 2e^{2v_t}|dw|^2$ on S_t converge to $I = 2e^{2v}|dw|^2$. Note that I is the induced metric on the maximal surface S corresponding to the polynomial $w^k dw^2$, thus we expect that the surfaces S_t converge to S and, consequently, the polygons on the boundary of S_t converge to the polygon on the boundary of S . Indeed, if we change coordinates from $z = x + iy$ to $w = \eta + i\zeta$ in Equations (3.1) and (3.2), we see that the coefficients of the new matrices $\hat{P}_t(v_t(w))$ and $\hat{Q}_t(v_t(w))$ such that

$$\begin{aligned}\partial_\eta \hat{\mathcal{F}}_t &= \hat{\mathcal{F}}_t \hat{P}_t \\ \partial_\zeta \hat{\mathcal{F}}_t &= \hat{\mathcal{F}}_t \hat{Q}_t,\end{aligned}$$

where $\hat{\mathcal{F}}_t$ is the matrix defined analogously to \mathcal{F} but using the coordinate w , converge to the coefficients of the corresponding matrices defined for the maximal surface S as t goes to $+\infty$. Thus the solution $\hat{\mathcal{F}}_t$ to the above ODEs converges to the frame of the maximal surface S . Since the parameterizations of the surfaces are obtained by taking the last column of these matrices, we deduce that S_t converges to S . This concludes the proof of Theorem A.

5. ACKNOWLEDGMENTS

We would like to thank Dr. Andrea Tamburelli for his suggestion of and invaluable assistance on this project. He introduced us to the world of anti-de Sitter geometry, and assisted us in understanding the background of the project. In addition, he provided suggestions whenever we were stuck, for which we are very grateful.

REFERENCES

- [Tam19] Andrea Tamburelli. “Polynomial quadratic differentials on the complex plane and light-like polygons in the Einstein Universe”. In: *Advances in Mathematics, Volume 352*, pp. 483-515 (2019).